Supporting Information for "High-latitude stratospheric aerosol injection to preserve the Arctic"

Walker Raymond Lee[1], Douglas G. MacMartin[1], Daniele Visioni[1], Ben Kravitz[2,3], Yating Chen[4], John C. Moore[4,5,6], Gunter Leguy[7], David M. Lawrence[7], David A. Bailey[7]

[1]Sibley School for Mechanical and Aerospace Engineering, Cornell University, Ithaca, NY, USA

[2]Department of Earth and Atmospheric Science, Indiana University, Bloomington, IN, USA

[3]Atmospheric Sciences and Global Change Division, Pacific Northwest National Laboratory, Richland, WA, USA

[4]College of Global Change and Earth System Science, Beijing Normal University, Beijing, 100875, China

[5]CAS Center for Excellence in Tibetan Plateau Earth Sciences, Beijing, 100101, China

[6]Arctic Centre, University of Lapland, Rovaniemi, Finland

[7]Climate and Global Dynamics Laboratory, National Center for Atmospheric Research, Boulder, CO, USA

Contents of this file

1. Text S1 and S2
2. Figures S1 to S5

Introduction Text S1 describes in more detail the feedforward/feedback control algorithm design process used to determine the injection rates for Arctic Low and Arctic High. Text S2 describes the statistical methods used to calculate standard error for multi-year averages for single simulations and ensenmbles with multiple members. Figures S1 and S2 show SW and LW fluxes; these figures are the same as Figures 2 and 3 in the manuscript, respectively, but with data for Arctic Low included. Figure S3 shows Atlantic Meridional Overturning Circulation (AMOC) data for Arctic Low, Arctic High, Global+1.5, and SSP2-4.5. Figure S4 shows column ozone changes as a function of season and latitude for Arctic High relative to SSP2-4.5. Figure S5 shows changes to Greenland for Arctic High relative to SSP2-4.5, including near-surface temperature, near-surface humidity, runoff, precipitation, and evaporation.

Text S1. The control algorithms used in the Arctic Low and Arctic High simulations consist of a feedforward term and a feedback term: the feedforward term, derived from previous simulations, estimates how much injection will be needed each year in order to meet the target September sea ice extent, and the feedback term applies a correction each year based on the difference between the actual and desired September sea ice extent during the simulation.

The feedforward gain is computed by estimating the linear increase in forcing needed to maintain the desired sea ice extent through our simulations. However, this is not as simple as finding the difference between sea ice in MAM-60 and RCP8.5 and dividing by injection rate because, during those simulations, the difference in sea ice extent is not proportional to changes in forcing; this is because September sea ice extent declines approximately linearly in 2000-2030 under RCP8.5 but nonlinearly by the MAM-60 simulation period of 2035-2045 (when September sea ice extent is close to 0). Therefore, in order for September sea ice differences in those simulations to be proportional to changes in forcing, we must extrapolate from the linear decline of 2000-2030 as in Lee, MacMartin, Visioni, and Kravitz (2020) and we compute a sensitivity of approximately 0.4 million km2 of sea ice restored per Tg of SO_2 injected (1 Tg = 1 Mt = 10^{12} g). This results in a feedforward gain of 0.272 Tg/yr for Arctic Low and 6.109 Tg + 0.272 Tg/yr for Arctic High (with the offset in the Arctic High case to account for the sea ice difference between the reference time period of 2000-2020 and the first year of the simulation).

The feedback gain is computed using the MATLAB system identification toolbox, which, when provided an "input" and an "output", can compute a relationship between them (referred to in feedback control theory as a "transfer function") and then can compute feedback gains that produce a desired response. We define the MAM-60 injection rate of 12 Tg/yr as the input and the difference in September sea ice extent between MAM-60 and RCP8.5 as the output, and we specify an integral controller with a time constant of five years; this is the same time constant as the original design of Kravitz et al. (2017) and has been subsequently used in Tilmes et al. (2018, 2020); Richter et al. (2022); and MacMartin et al. (2022). This process computes a feedback gain of 0.491 Tg per year per million km^2, which is used in both Arctic Low and Arctic High (i.e., the injection quantity each year is adjusted up or down by 0.491 Tg for each million km^2 of the total time-integrated difference between model output and the target).

Text S2. 20-year averages are reported in the manuscript as $\mu \pm \delta$, where μ is the average and δ is the standard error. To compute the standard error for the 20-year average of a discrete timeseries, we approximate the timeseries y(t) as a first-order autoregression, or AR(1), to account for interannual autocorrelation. An AR(1) approximation is given by the standard formula

$$y(t) = \beta_0 + \beta 1 y(t-1) + \epsilon_t \tag{1}$$

where β_0 is a constant, β_1 is the correlation coefficient between y(t) and y(t-1), and ϵ_t is random noise. After computing β_0 and β_1, we solve for ϵ for the latter 19 years of data using the above equation. We then compute

$$\delta = \sigma_\epsilon / \sqrt{(n_y - 1)} \tag{2}$$

where σ_ϵ is the standard deviation of the noise and $(n_y - 1) = 20 - 1 = 19$ degrees of freedom after the interannual autocorrelation has been removed.

For a simulation with multiple ensemble members, δ_{ens} for a 20-year average for the entire ensemble is a function of δ for each of the individual ensemble members. This is done using the standard error propagation formula

$$\delta_{ens} = \frac{\sqrt{\delta_1^2 + ... + \delta_{n,ens}^2}}{n_{ens}} \tag{3}$$

with n_{ens} equal to the number of ensemble members (note that for an ensemble size of 1, $\delta = \delta_{ens}$). For a 20-year average of the difference between two ensemble members, δ_{diff} is found using the same error propagation formula

$$\delta_{diff} = \sqrt{\delta_{ens,1}^2 + \delta_{ens,2}^2} \tag{4}$$

Therefore, to compute (for example) the change in FSNT between Arctic High and SSP2-4.5 during the 2050-2069 period, as seen in Fig. 2a in the manuscript, we first compute the 20-year δ individually for the one ensemble member of Arctic High and each of the three ensemble members of SSP2-4.5 using Eqns. 1 and 2. We then compute δ_{ens} for SSP2-4.5 using Eqn. 3 with δ from each of the three ensemble members. Lastly, we compute δ_{diff} using Eqn. 4 with $\delta = \delta_{ens}$ for the one ensemble member of Arctic High and δ_{ens} for SSP2-4.5.

References

Kravitz, B., MacMartin, D. G., Mills, M. J., Richter, J. H., Tilmes, S., Lamarque, J.-F., ... Vitt, F. (2017). First Simulations of Designing Stratospheric Sulfate Aerosol Geoengineering to Meet Multiple Simultaneous Climate Objectives. *Journal of Geophysical Research: Atmospheres*, *122*(23), 12,616-12,634. doi: 10.1002/2017JD026874

Lee, W., MacMartin, D., Visioni, D., & Kravitz, B. (2020). Expanding the design space of stratospheric aerosol geoengineering to include precipitation-based objectives and explore trade-offs. *Earth System Dynamics*, *11*(4), 1051–1072. doi: 10.5194/esd-11-1051-2020

MacMartin, D. G., Visioni, D., Kravitz, B., Richter, J. H., Felgenhauer, T., Lee, W. R., ... Sugiyama, M. (2022). Scenarios for modeling solar radiation modification. *Proceedings of the National Academy of Sciences of the United States of America.*

Richter, J., Visioni, D., MacMartin, D., Bailey, D., Rosenbloom, N., Lee, W., ... Lamarque, J.-F. (2022). Assessing responses and impacts of solar climate intervention on the earth system with stratospheric aerosol injection (arise-sai). *EGUsphere*, *2022*, 1–35. doi: 10.5194/egusphere-2022-125

Tilmes, S., MacMartin, D. G., Lenaerts, J. T. M., van Kampenhout, L., Muntjewerf, L., Xia, L., ... Robock, A. (2020). Reaching 1.5 and 2.0°C global surface temperature targets using stratospheric aerosol geoengineering. *Earth System Dynamics*, *11*(3), 579–601. doi: 10.5194/esd-11-579-2020

Tilmes, S., Richter, J. H., Kravitz, B., MacMartin, D. G., Mills, M. J., Simpson, I. R.,

. . . Ghosh, S. (2018, 12). CESM1(WACCM) Stratospheric Aerosol Geoengineering Large Ensemble Project. *Bulletin of the American Meteorological Society*, *99*(11), 2361-2371. doi: 10.1175/BAMS-D-17-0267.1

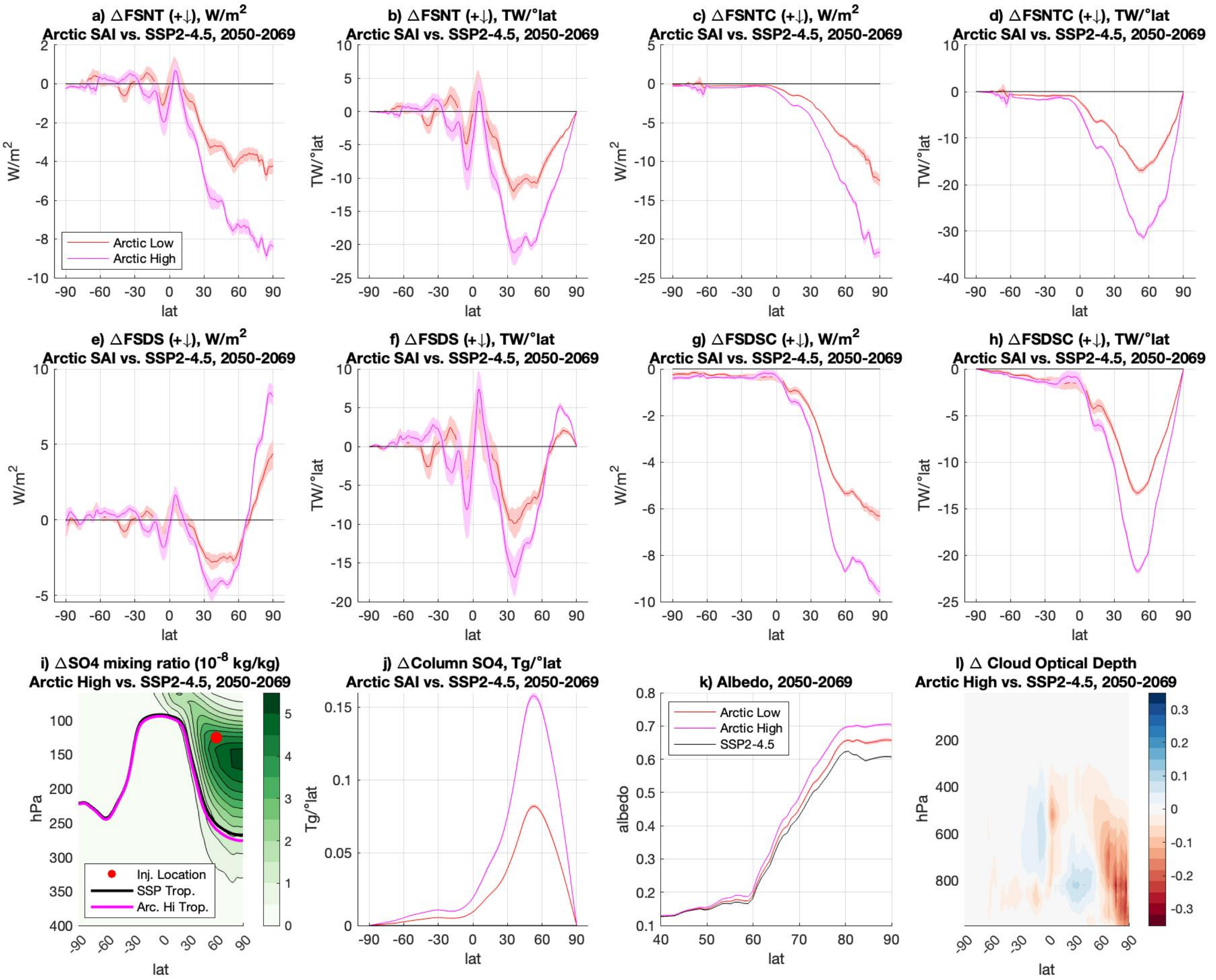

Figure S1. Changes to shortwave (SW) fluxes, sulfur burden, surface albedo, and cloud optical depth. This figure is identical to Fig. 2 in the manuscript, but with Arctic Low included for panels a-h and j-k.

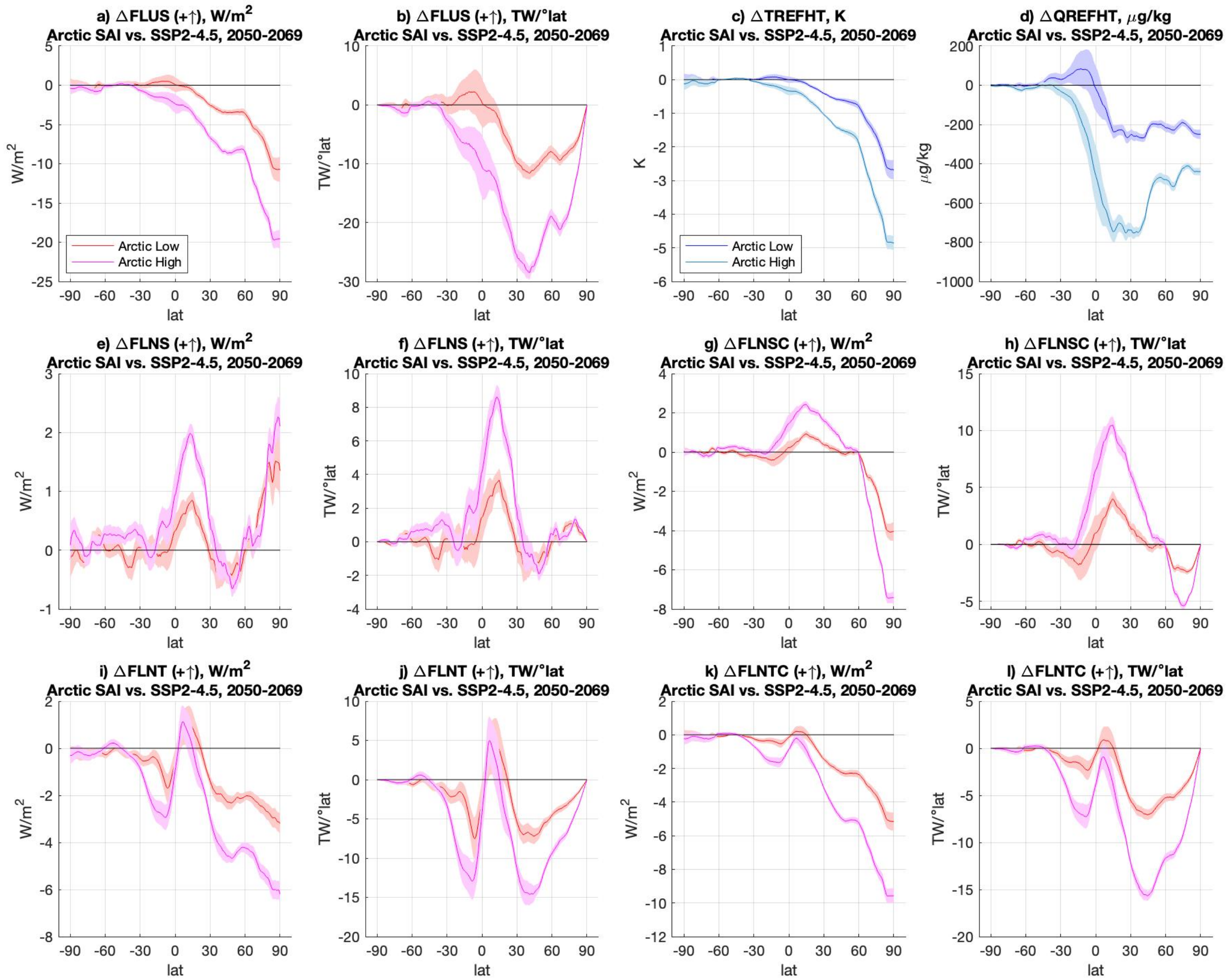

Figure S2. Changes to shortwave (LW) fluxes, surface temperature, and near-surface humidity. This figure is identical to Fig. 3 in the manuscript, but with Arctic Low included for all panels.

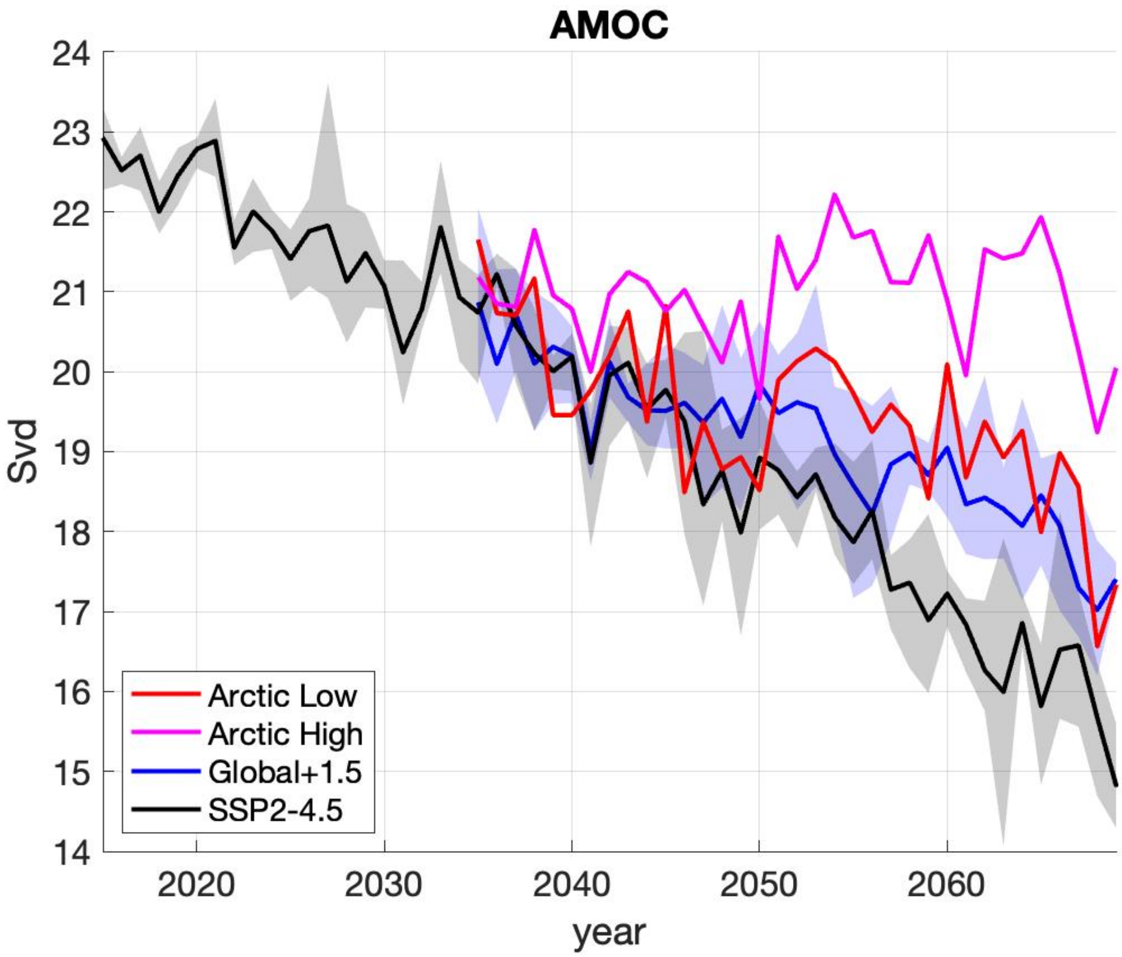

Figure S3. Strength of the Atlantic Meridional Overturning Circulation (AMOC) over time for Arctic SAI, Global+1.5, and SSP2-4.5. Shading for Global+1.5 and SSP2-4.5 denotes ensemble spread.

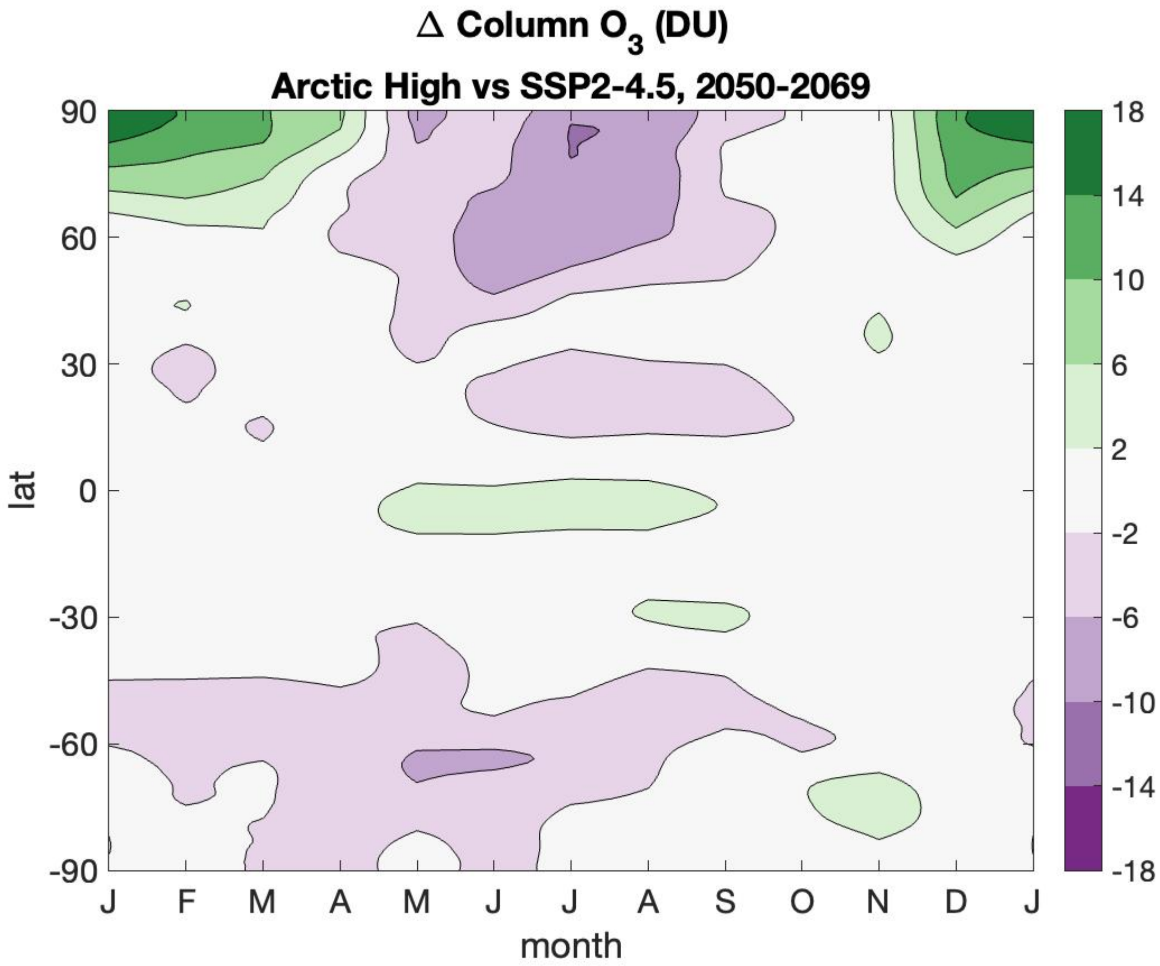

Figure S4. Changes to the zonal mean seasonal cycle of atmospheric column ozone burden for Arctic High relative to SSP2-4.5, averaged over the 2050-2069 period.

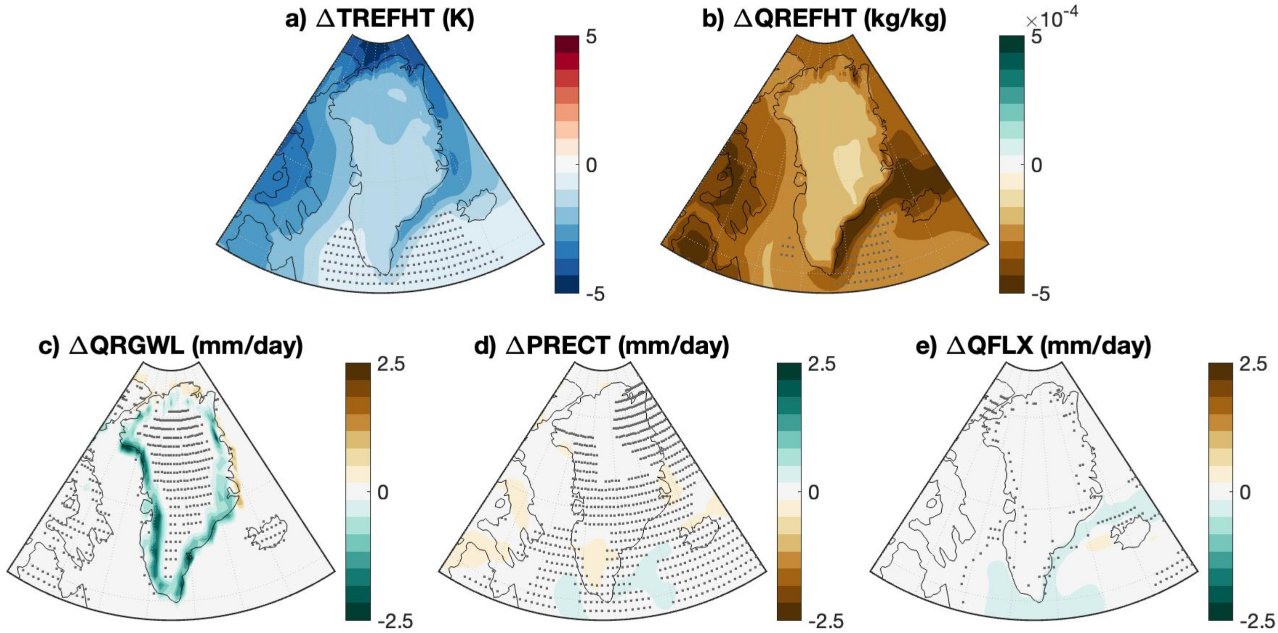

Figure S5. Maps of changes to near-surface temperature (a), near-surface humidity (b), runoff (c), precipitation (d), and evaporation (e) for Arctic High relative to SSP2-4.5, averaged over the 2050-2069 period. Stippling indicates areas with no significant change according to the two-sample t-test at the 95% confidence level.